processes

MDPI

Article

Screening of Metal Reduction Potential for Thermochemical Hydrogen Storage

Jure Voglar [1,*] and Blaž Likozar [1,2,3,4,*]

[1] Department of Catalysis and Chemical Reaction Engineering, National Institute of Chemistry, Hajdrihova 19, 1001 Ljubljana, Slovenia
[2] Faculty of Chemistry and Chemical Technology, University of Ljubljana, Večna pot 113, 1001 Ljubljana, Slovenia
[3] Faculty of Chemistry and Chemical Engineering, University of Maribor, Smetanova ulica 17, 2000 Maribor, Slovenia
[4] Faculty of Polymer Technology, Ozare 19, 2380 Slovenj Gradec, Slovenia
* Correspondence: jure.voglar@ki.si (J.V.); blaz.likozar@ki.si (B.L.)

Abstract: The screening of all non-radioactive metals without lanthanides for thermochemical hydrogen storage was performed based on physical chemistry calculations. The thermodynamic data were collected from the NIST (National Institute of Standards and Technology) public data repository, which was followed by calculations regarding the change in enthalpy, entropy, Gibbs free energy and equilibrium reaction temperature. The results were critically evaluated based on thermodynamic parameters, viable metals were identified, and their hydrogen storage densities and energy–enthalpy ratios were evaluated. The elements viable for controlled thermochemical hydrogen storage via the reversible reduction and oxidation of metal oxides and metals are manganese (Mn), iron (Fe), molybdenum (Mo) and tungsten (W). Manganese has the largest theoretical potential for hydrogen storage with reversible reduction and oxidation of metal oxides and metals. The second candidate is iron, while the other two (Mo and W) have much lower potential. More research efforts should be dedicated to experimental testing of the identified metals (Mn, Fe, Mo and W) and their different oxides for thermochemical hydrogen storage capabilities both on laboratory and pilot scales. Ferromanganese alloy(s) might also prove itself as an efficient and affordable thermochemical hydrogen storage material. Our theoretical investigation expanded the knowledge on thermochemical hydrogen storage and is accompanied with a brief literature review revealing the lack of experimental studies, especially on oxidation of metals with water vapor occurring during the hydrogen release phase of the cycle. Consequently, accurate modelling of transport, kinetics and other phenomena during hydrogen storage and release is scarce.

Keywords: hydrogen storage; reduction and oxidation; metals; physical chemistry calculations; screening

Citation: Voglar, J.; Likozar, B. Screening of Metal Reduction Potential for Thermochemical Hydrogen Storage. *Processes* **2024**, *12*, 1004. https://doi.org/10.3390/pr12051004

Academic Editor: Paola Ammendola

Received: 8 April 2024
Revised: 8 May 2024
Accepted: 13 May 2024
Published: 15 May 2024

1. Introduction

Since hydrogen will act as an energy buffer [1] in the future decarbonized society where the majority of power sources are intermittent, e.g., wind power plants, its effective and efficient storage will play an important role in adoption of the hydrogen economy by the energy sector. Hydrogen can be stored in multiple manners e.g., compressed hydrogen, liquefied hydrogen, cryocompressed hydrogen, physically adsorbed hydrogen, metal hydrides, complex hydrides, liquid organic hydrogen carriers (LOHC) or liquid organic hydrides [2,3]. On the other hand, hydrogen can also be converted into other hydrogen-containing compounds, e.g., ammonia [4] and methanol [5], and stored. Another way to store hydrogen is by the reduction of selected metal oxides and its subsequent release by metal oxidation with water vapor, which is known as the reversible reduction

and oxidation of metal oxides [6]. This thermochemical storage method is schematically presented in Figure 1.

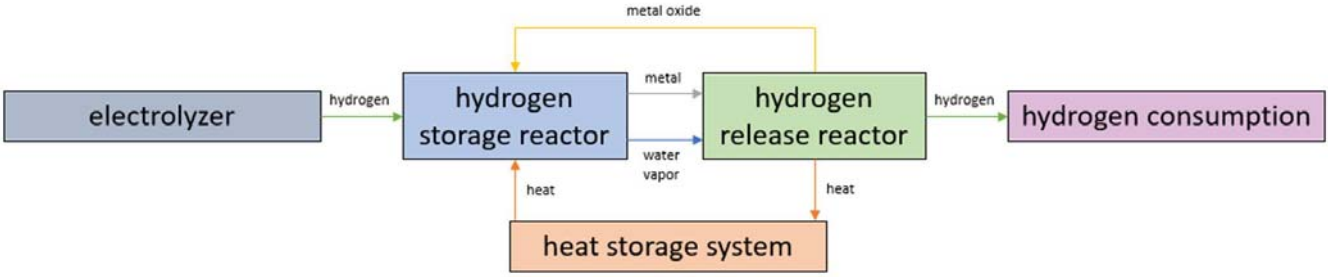

Figure 1. Schematic representation of thermochemical hydrogen storage with reversible reduction and oxidation of metal oxides combined with heat storage system.

Brinkman et al. [6] listed six different metal oxide/metal pairs for thermochemical hydrogen storage: Fe_3O_4/Fe, ZnO/Zn, SnO_2/SnO, GeO_2/Ge, $WO_{2.722}$/W and MoO_2/Mo. They stated that the pairs were chosen because their change in the standard Gibbs free energy of the reduction reaction allows for a reversible redox process at reasonable temperatures. Their physical chemistry calculations were made with two aims: (i) minimal 10% conversion of the hydrogen during reduction and (ii) at least 50% conversion of the steam during oxidation. The conversion extent was identified as more critical during oxidation, since excess unreacted steam is energetically expensive to produce and must be later condensed out of the product to extract pure hydrogen. They identified zinc and tin as unfavorable candidates from the perspective of process conditions. Germanium and iron have the highest gravimetric storage densities with germanium being too expensive (for most of the applications). This analysis has left us with three viable metal oxide/metal pairs: Fe_3O_4/Fe, $WO_{2.722}$/W and MoO_2/Mo. They also concluded the raw material cost of all options besides Fe_3O_4/Fe and ZnO/Zn is higher than the estimated cost of a gaseous hydrogen storage vessel. Considering all these aspects, iron oxide (Fe_3O_4/Fe) was selected as a promising candidate for hydrogen storage and was further studied in their article [6].

Iron (Fe) has been and is studied the most for the purpose of thermochemical hydrogen storage [7–10]. Efforts [7,8] in improving activity and stability (resistance to sintering) of the solids (metals and their oxides) along multiple cycles have been made by the addition of other metals, e.g., Al and Ce to iron.

Otsuka et al. [7] tested the reduction and oxidation of the iron oxide samples with various metal additives in a conventional gas flow system with a fixed bed at a gas mixture pressure of 101 kPa and flow rate of 100 mL/min (at standard temperature and pressure, STP). The reduction experiments were performed by heating the sample from 563 to 823 K with a rate of 7.5 K/min while maintaining a steady stream of 50:50 vol% gas mixture of hydrogen and argon, respectively. After the temperature reached 823 K, this temperature was maintained until the consumption of hydrogen stopped. The oxidation of the reduced samples by water vapor followed after the reduction experiments. The reduced sample was cooled to room temperature, and the remaining hydrogen was purged with argon out of the system. The oxidation was initiated with a steady stream of 5:95 vol% of water vapor and argon mixture, respectively. Simultaneously, the temperature of the bed increased from 373 to 873 K with a rate of 4 K/min. After it reached 873 K, the temperature was kept at this temperature until hydrogen formation ceased. Al, Mo and Ce were favorable metal additives for preserving the Fe/Fe_3O_4 sample from decaying its reactivity by repeated cycles.

Lorente et al. [8] performed isothermal experiments of reduction with hydrogen-rich flows and oxidation with steam with Al, Cr and Ce as second metals in nominal amounts from 1 to 10 mol% added to the hematite. The experiments were performed in a thermobalance with a sample mass of 20.0 mg, a sieve fraction of 100–160 µm, a total gas flow rate of 750 mL/min (STP), temperature of 450 °C and at atmospheric pressure.

A gas mixture of 50:50 vol% of hydrogen and nitrogen was used for the reduction step. The remaining gases were then purged with nitrogen. In the oxidation step, a mixture of steam and nitrogen was fed at the partial pressure of steam equal to 0.2 bar. The reduction–oxidation cycles were repeated seven times. The addition of Al, Cr and Ce to the iron oxide greatly improved the stability and oxidation activity of the solids during the repeated reduction–oxidation cycles. For all cases, an optimum percentage of metal additive (around 5 mol%) could be found, for which the maximal hydrogen storage density was measured and remained practically constant along the cycles. However, the reduction kinetics was slowed down with additions of Al and Cr, while it remained similar by adding Ce compared to pure iron oxide.

At present, a group of students are working on Iron-based Hydrogen Storage (IRHYS) technology, which offers an alternative to existing hydrogen storage options [9]. They are trying to show proof of concept, build a reactor, optimize the process and make IRHYS technology economically feasible.

Recently, kinetic mechanisms of the reduction–oxidation reactions of iron oxide–iron pellets under different operating conditions were investigated by Gamisch et al. [10]. A single pellet consisting of iron oxide (90% Fe_2O_3, 10% stabilizing cement) was reduced with different hydrogen concentrations at temperatures between 600 and 800 °C. Oxidation of the previously reduced pellet was initiated by the introduction of water vapor at different concentrations in the same temperature range. Nitrogen was used as a carrier gas, while flow rates of gas mixtures were kept at 250 mL/min. With application of the shrinking core reaction mechanism model, the concentration- and temperature-dependent reduction and oxidation rates were accurately reproduced. The activation energies of reduction and oxidation were found to be 56.9 and 16.0 kJ/mol, respectively.

Thaler and Hacker [11] considered 18 different metals and their corresponding oxides for their potential as thermochemical hydrogen storage material and concluded that Ge, Mo, W and Fe are potential candidates for the separation process with high hydrogen concentration in the product gas and excellent reduction and oxidation capability. Their isothermal thermogravimetric experiments of reduction of metal oxides with pure hydrogen and the later oxidation of metals with water vapor at temperatures of 670 °C ($MoO_2 \leftrightarrow Mo$), 620 °C ($GeO_2 \leftrightarrow Ge$), 720 °C ($WO_3 \leftrightarrow W$) and 800 °C ($Fe_2O_3 \leftrightarrow Fe$) demonstrated the practical feasibility of the processes. The first step of reduction of the metal oxides with hydrogen was successful in all four cases and led to complete reduction within 15 min. However, they discovered that the re-oxidation part of the experiment led to only partial oxidation within 20 min with the exception of tungsten, which almost completely re-oxidized within the same timeframe. The slower reaction rate of re-oxidation most likely originates from the sintering of the samples, since iron, germanium and molybdenum were visibly sintered after just one cycle of operation. The slow oxidation reactions could be at least partially compensated with (i) taking a longer time for the process of re-oxidation to be (more) complete, (ii) changing the process parameters, e.g., temperature, gas flow rate, (iii) replacing the rector (type and/or size), (iv) grinding the materials between the reduction/oxidation phases of the thermochemical hydrogen storage cycle and (v) adding a small amount of other metal(s), which increases the thermal stability of the material. Some combination of the previously stated measures might also favor the re-oxidation process.

Our work includes the theoretical screening of all non-radioactive metals without lanthanides and their respective oxides based on physical chemistry calculations for a reversible reduction and oxidation of metal oxides. We selected only non-radioactive metal elements since we wanted the materials to be stable hydrogen storage materials while the lanthanides were excluded, since they are high-value commodities which will be used in the green energy transition and will be better utilized in various different devices, e.g., wind turbine generators. The main goal was to find the potential candidates (metals) which would theoretically enable thermochemical hydrogen storage with the reversible reduction and oxidation of metal oxides and metals.

2. Methods

All of the non-radioactive elements of metals with the exception of the lanthanides (45 elements) were systematically screened for their potential as thermochemical hydrogen storage material via the reversible reduction and oxidation of metal oxides and metals, respectively (Figure 2). The screening itself consisted of the following: (i) selection of metal oxides (in stable form), (ii) retrieval of thermodynamic and other relevant (e.g., melting point) properties of metals and the selected metal oxides, (iii) physical chemistry calculations of metal oxide reduction reactions, (iv) feasibility evaluation based on physical chemistry calculation results, (v) hydrogen storage performance evaluation of the viable materials and (vi) estimation of the potential for thermochemical hydrogen storage.

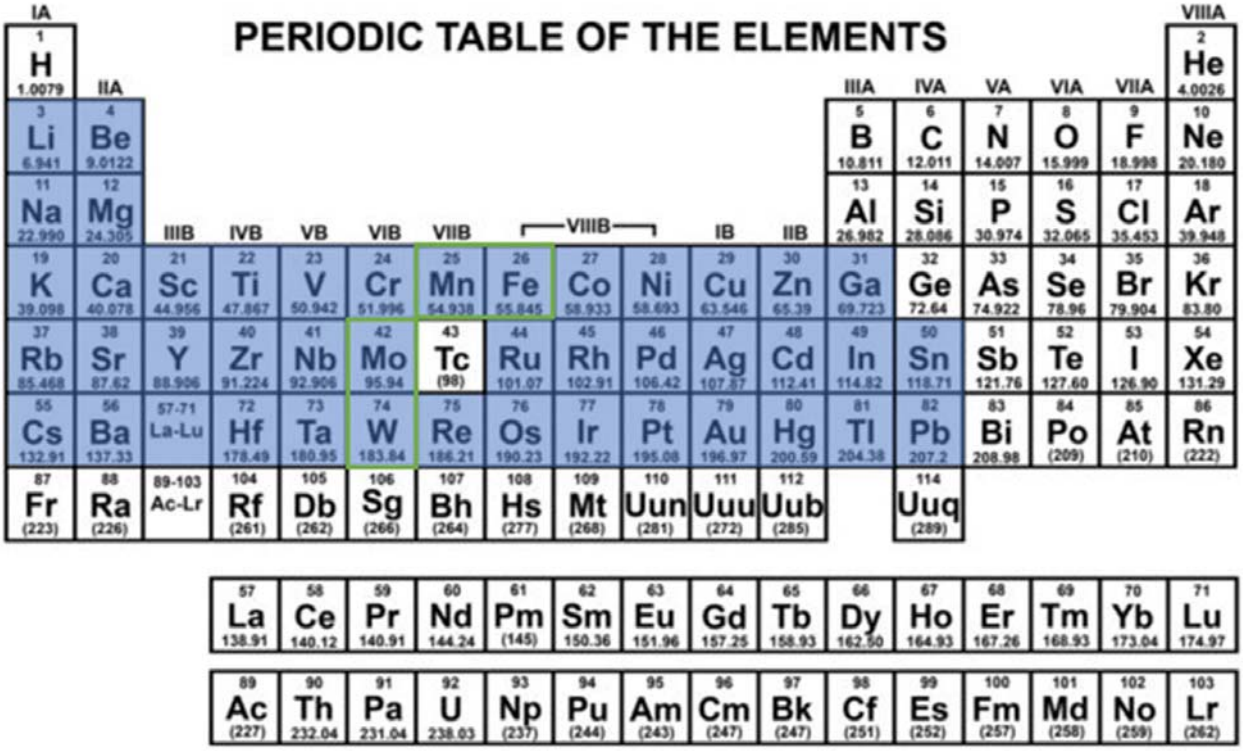

Figure 2. Periodic table of the elements with presentation of the screened elements for thermochemical hydrogen storage (colored blue) and the four viable elements based on physical chemistry calculations (green outline).

Thermochemical hydrogen storage follows the reactions of reversible reduction of metal oxides (Me_xO_y) during the hydrogen storage phase and oxidation of metals (Me) during the hydrogen release phase, which are shown below:

$$Me_xO_y(s) + yH_2(g) \leftrightarrow xMe(s,l \text{ for Hg}) + yH_2O(g) \quad (1)$$

The values of molar mass (M), standard enthalpy of formation ($\Delta_f H^o$), standard molar entropy (S^o) and the melting point temperature (T_m) are presented for both the selected metals (Table 1) and their corresponding oxides (Table 2). The thermodynamic data originate from the NIST (National Institute of Standards and Technology) public data repository [12].

Table 1. Standard thermodynamic values for the selected metals.

Metal	M (g/mol)	$\Delta_f H^o$ (kJ/mol)	S^o (J/(K·mol))	T_m (°C)
Li	6.941	0	160.7	180.5
Be	9.012	0	9.5	1287
Na	22.990	0	51.5	97.8
Mg	24.305	0	32.7	650
Al	26.982	0	28.3	660.32
K	39.098	0	64.7	63.5
Ca	40.078	0	41.4	842
Sc	44.956	0	34.6	1541
Ti	47.867	0	30.7	1668
V	50.942	0	28.9	1910
Cr	51.996	0	23.6	1907
Mn	54.938	0	32.0	1246
Fe	55.845	0	27.3	1538
Co	28.010	0	30.0	1495
Ni	58.693	0	29.9	1455
Cu	63.546	0	33.1	1084.62
Zn	65.380	0	41.6	419.53
Ga	69.723	0	40.8	29.76
Rb	85.468	0	69.5	39.3
Sr	87.620	0	52.3	777
Y	88.906	0	44.4	1522
Zr	91.224	0	39.0	1855
Nb	92.906	0	36.5	2477
Mo	95.960	0	28.6	2623
Ru	101.070	0	28.5	2334
Rh	102.906	0	31.5	1964
Pd	106.420	0	37.6	1554.8
Ag	107.868	0	42.6	961.78
Cd	112.411	0	51.8	321.07
In	114.818	0	57.8	156.6
Sn	118.710	0	51.5	231.93
Cs	132.905	0	85.1	28.44
Ba	137.327	0	62.3	727
Lu	174.967	0	51.0	1652
Hf	178.490	0	43.6	2233
Ta	180.948	0	41.5	3017
W	183.840	0	32.7	3422
Re	186.207	0	36.9	3185
Os	190.230	0	32.6	3033

Table 1. *Cont.*

Metal	M (g/mol)	$\Delta_f H^o$ (kJ/mol)	S^o (J/(K·mol))	T_m (°C)
Ir	192.217	0	35.5	2446
Pt	195.084	0	41.6	1768.2
Au	196.967	0	47.4	1064.18
Hg	200.590	0	76.0	−38.83
Tl	204.383	0	64.2	304
Pb	207.200	0	64.8	327.46

Table 2. Standard thermodynamic values for the selected metal oxides.

Oxide	M (g/mol)	$\Delta_f H^o$ (kJ/mol)	S^o (J/(K·mol))	T_m (°C)
Li_2O	29.881	−595.8	37.9	1438
BeO	25.012	−609.4	13.8	2578
Na_2O	61.979	−416.0	73.0	1132
MgO	40.304	−601.6	27.0	2852
Al_2O_3	101.961	−1675.7	50.9	2072
K_2O	94.196	−363.2	94.0	740
CaO	56.077	−635.0	40.0	2613
Sc_2O_3	137.910	−1908.8	77.0	2485
TiO_2	79.866	−945.0	50.0	1843
V_2O_5	181.880	−1550.6	131.0	681
Cr_2O_3	151.990	−1128.0	81.0	2435
MnO_2	86.937	−520.0	53.1	535
Fe_2O_3	159.688	−824.2	87.4	1539
Co_3O_4	148.028	−910.0	114.4	895
NiO	74.693	−240.0	38.0	1955
CuO	79.545	−156.0	43.0	1326
ZnO	81.379	−350.5	43.7	1974
Ga_2O_3	187.444	−1089.1	85.0	1725
Rb_2O	186.935	−339.0	126.0	500
SrO	103.619	−592.0	57.2	2531
Y_2O_3	225.810	−1905.3	99.1	2425
ZrO_2	123.223	−1080.0	50.3	2715
NbO	108.906	−405.9	48.1	1937
MoO_2	127.959	−588.9	46.3	1100
RuO_4	165.068	−239.3	146.4	25.4
Rh_2O_3	253.809	−405.5	75.7	1100
PdO	122.419	−112.7	39.6	750
Ag_2O	231.736	−31.0	122.0	300
CdO	128.410	−258.0	55.0	950
In_2O_3	277.634	−925.8	104.2	1910
SnO_2	150.709	−577.6	49.0	1630

Table 2. *Cont.*

Oxide	M (g/mol)	$\Delta_f H^o$ (kJ/mol)	S^o (J/(K·mol))	T_m (°C)
Cs_2O	281.810	−345.8	146.9	490
BaO	153.326	−582.0	70.0	1923
Lu_2O_3	397.932	−1878.2	110.0	2490
HfO_2	210.489	−1144.7	59.3	2758
Ta_2O_5	441.893	−2046.0	143.1	1872
WO_3	231.838	−842.9	75.9	1473
Re_2O_7	484.410	−1240.1	207.1	360
OsO_4	254.228	−394.1	143.9	40.25
IrO_2	224.216	−274.1	80.4 *	1100
PtO_2	227.083	171.5	80.4 *	450
Au_2O_3	441.931	−13.0	80.4 *	298
HgO	216.589	−90.0	70.0	500
Tl_2O	424.766	−178.7	126.0	596
PbO	223.199	−219.0	66.5	888

* The values of the standard molar entropy were estimated to be equal to 80.4 J/(K·mol) based on the mean value of the other metal oxides, since the missing three values were not found in the literature.

The reactions of reversible reduction and oxidation of metal oxides and metals were evaluated with physical chemistry calculations [13]. The hydrogen gas has the values of standard enthalpy of formation ($\Delta_f H^o$) and standard molar entropy (S^o) equal to 0 kJ/mol and 130.68 J/(K·mol), respectively. The water vapor has the values of standard enthalpy of formation ($\Delta_f H^o$) and standard molar entropy (S^o) equal to −241.83 kJ/mol and 188.84 J/(K·mol), respectively.

The reactions in the direction to the right (reduction of the metal oxide with gaseous hydrogen) were considered, and the changes in enthalpy (ΔH^o), entropy (ΔS^o), Gibbs free energy (at 298.15 K, ΔG^o) and the equilibrium reaction temperatures (T_{eq}) were calculated with the following equations:

$$\Delta H^o = H^o{}_{final} - H^o{}_{initial} \quad (2)$$

$$\Delta S^o = S^o{}_{final} - S^o{}_{initial} \quad (3)$$

$$\Delta G^o = \Delta H^o - T\Delta S^o \quad (4)$$

$$T_{eq} = \frac{\Delta H^o}{\Delta S^o} \quad (5)$$

The results were evaluated in terms of feasibility for thermochemical hydrogen storage in realistic conditions. After, that the viable materials were characterized in their hydrogen storage capacities. The two hydrogen storage densities were determined as follows:

$$SD_1 = \frac{yM_{H_2}}{xM_{Me}} \quad (6)$$

$$SD_2 = \frac{yM_{H_2}}{xM_{Me} + yM_{H_2O}} \quad (7)$$

The first one (SD_1) considers only the mass of the metal, while the second one (SD_2) also takes into account the mass of the water vapor.

The ratio of energy stored with hydrogen as its higher heating value (HHV_{H2}) of 285.8 kJ/mol [14] to reduction reaction enthalpy (stored heat) was also examined and marked as *EER* (energy–enthalpy ratio):

$$EER = \frac{yHHV_{H2}}{\Delta H^o} \quad (8)$$

Higher values of *EER* are desirable for efficient hydrogen storage, since a larger proportion of the stored energy is actually contained in hydrogen compared to heat. It is worth pointing out that the heat required to produce the water vapor (from water at 25 °C) required for hydrogen release represents circa one-sixth of the higher heating value of the stored hydrogen, which is valid for all possible metal oxide/metal pairs following the reaction (1).

By consideration of the thermodynamics, hydrogen storage capacity and energy–enthalpy ratio, the viable materials for thermochemical hydrogen storage via reversible reduction and oxidation were identified, and their potential was evaluated.

3. Results and Discussion

After performing the physical chemistry calculations, the results (Table 3) were critically evaluated. If the equilibrium reaction temperature (T_{eq}) was below the melting points of both the metal and its considered oxide, a tick mark was added to the metal as being a potentially viable option for thermochemical hydrogen storage via the reversible reduction and oxidation of metal oxides and metals, since we wish to avoid any loss of materials via evaporation (from liquid metal and metal oxide). The potentially viable metals according to this criterium are Mn, Fe, Co, Ni, Cu, Mo, Ru, Rh, Pd, Ag, Cd, W, Re, Os, Ir, Pt, Au, Hg, Tl and Pb (20 elements with tick marks in the Table 3). Among those, only four elements have equilibrium reduction reaction temperatures above 25 °C: Mn, Fe, Mo and W (green tick marks in the Table 3). Therefore, their oxides would not spontaneously react with hydrogen at room temperature.

Table 3. Calculated reduction reaction parameters.

Metal	ΔH^o (kJ/mol)	ΔS^o (J/(K·mol))	ΔG^o (kJ/mol)	T_{eq} (°C) *	Solid Metal and Oxide
Li	354.0	341.6	252.1	763.1	
Be	367.6	53.9	351.5	6542.6	
Na	174.2	88.1	147.9	1704.1	
Mg	359.8	63.9	340.7	5356.7	
Al	950.2	180.2	896.5	4999.6	
K	121.3	93.5	93.5	1024.6	
Ca	393.2	59.6	375.4	6325.7	
Sc	1183.3	166.7	1133.6	6826.3	
Ti	461.3	97.0	432.4	4483.5	
V	341.5	217.7	276.6	1295.6	
Cr	402.5	140.7	360.6	2587.3	
Mn	36.3	95.2	7.9	108.5	✓
Fe	98.7	141.6	56.5	423.8	✓
Co	−57.3	208.3	−119.4	−548.2	✓
Ni	−1.8	50.0	−16.8	−309.7	✓
Cu	−85.8	48.3	−100.2	−2049.8	✓
Zn	108.6	56.1	91.9	1661.8	

Table 3. *Cont.*

Metal	ΔH^o (kJ/mol)	ΔS^o (J/(K·mol))	ΔG^o (kJ/mol)	T_{eq} (°C) *	Solid Metal and Oxide
Ga	363.6	171.1	312.6	1851.5	
Rb	97.2	71.1	76.0	1094.1	
Sr	350.2	53.3	334.3	6301.6	
Y	1179.8	164.3	1130.8	6909.5	
Zr	596.3	105.0	565.0	5405.2	
Nb	164.0	46.5	150.1	3251.9	
Mo	105.3	98.6	75.9	794.2	✓
Ru	−728.0	114.8	−762.2	−6616.4	✓
Rh	−320.0	161.8	−368.2	−2250.5	✓
Pd	−129.1	56.2	−145.9	−2571.8	✓
Ag	−210.8	21.3	−217.2	−10188.7	✓
Cd	16.2	54.9	−0.2	21.3	✓
In	200.3	185.9	144.9	804.2	
Sn	94.0	118.8	58.5	517.7	
Cs	104.0	81.5	79.7	1001.8	
Ba	340.2	50.5	325.1	6462.7	
Lu	1152.7	166.4	1103.1	6652.5	
Hf	661.0	100.6	631.1	6301.1	
Ta	836.9	230.7	768.1	3354.0	
W	117.4	131.3	78.3	621.4	✓
Re	−452.7	273.7	−534.3	−1926.9	✓
Os	−573.2	121.3	−609.4	−4997.2	✓
Ir	−209.6	71.4	−230.8	−3208.2	✓
Pt	−655.2	77.6	−678.3	−8721.4	✓
Au	−712.5	188.9	−768.8	−4045.1	✓
Hg	−151.8	64.2	−171.0	−2638.7	✓
Tl	−63.1	60.5	−81.2	−1316.3	✓
Pb	−22.8	56.4	−39.7	−678.1	✓

* We are well aware that the equilibrium temperatures below absolute zero (−273.15 °C) could not be achieved and are just a result of the calculations.

According to our physical chemistry calculations, the elements viable for controlled thermochemical hydrogen storage via the reversible reduction and oxidation of metal oxides are manganese (Mn), iron (Fe), molybdenum (Mo) and tungsten (W). In all four cases (Mn, Fe, Mo and W), hydrogen storage (reduction of metal oxide) is an endothermal process ($\Delta H^o > 0$ in Table 3), while hydrogen release (oxidation of metal) is an exothermal process. Therefore, the heat could be in cases where the hydrogen storage/release cycle is not too long (up to 2 weeks, [15]) stored [16] during hydrogen (and heat) release and released during hydrogen (and heat) storage.

Figure 3 presents the Gibbs free energy dependence on temperature for the hydrogen reduction of MnO_2, Fe_2O_3, MoO_2 and WO_3 to Mn, Fe, Mo and W, respectively.

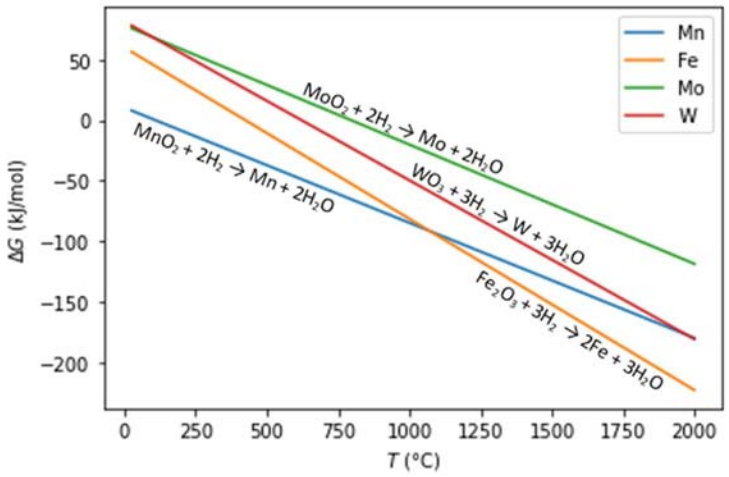

Figure 3. Gibbs free energy for complete hydrogen reduction of MnO_2, Fe_2O_3, MoO_2 and WO_3.

The reduction of MnO_2 to MnO is feasible below 1000 °C (Barner and Mantell [17] studied it in the range from 200 to 500 °C), while the conversion from MnO to metal (Mn) would require much higher temperature (above the melting point of Mn) and low water vapor content in the gas phase (at p_{H2O}/p_{H2} ratio below 3×10^{-4}). However, multiple experimental studies [17–20] reported the fact that MnO_2 cannot be reduced fully into metallic Mn but rather into suboxides, following the reaction sequence: $MnO_2 \rightarrow Mn_2O_3 \rightarrow Mn_3O_4 \rightarrow MnO$. This is supported by the work of Thaler and Hacker [11], where MnO was identified as a stable metal oxide. Autocatalytic behavior was found on Mn_3O_4 reduction by Tatievskaya et al. [21]. Whether MnO can be completely reduced by hydrogen to Mn (or just to MnO), and at which process conditions this could take place, should be thoroughly investigated.

The temperature-programmed reduction (TPR) of Fe_2O_3 in the 5.8% H_2, 1.2% H_2O, Ar mixture to iron (Fe) terminated at 970 °C [22]. Zieliński et al. [22] found three possible routes for the reduction of hematite, which mainly depend on the water vapor content. When there is no water vapor (or if it is present in extremely low concentrations), the reduction reaction follows: $Fe_2O_3 \rightarrow Fe$. If the water vapor to hydrogen molar ratio is below 0.35, the reaction is $Fe_2O_3 \rightarrow Fe_3O_4 \rightarrow Fe$. In case the water vapor to hydrogen molar ratio is above 0.35, the reduction reaction is $Fe_2O_3 \rightarrow Fe_3O_4 \rightarrow FeO \rightarrow Fe$. Temperature is also influencing the hematite reduction sequence, since below 570 °C, it follows: $Fe_2O_3 \rightarrow Fe_3O_4 \rightarrow Fe$, while above 570 °C, we can observe the sequence: $Fe_2O_3 \rightarrow Fe_3O_4 \rightarrow FeO \rightarrow Fe$ [23]. Fine iron ore was reduced in a fluidized bed reactor [24]. The sticking of fine iron ore particles is identified as a problem causing interruptions to the reduction process [25]. The reduction of iron ore should take place at the temperature above 420 °C, while above 570 °C, Wüstite (FeO) formation is favorable as an intermediate product [6]. The direct reduction of iron oxides is governed by mechanisms stemming from a complex interaction of several chemical (phase transformations), physical (transport), and mechanical (stresses) phenomena [23]. Natural iron ores were considered by Bock et al. [26] as an inexpensive storage material for large-scale mid- and long-term energy storage via reversable reduction and metal oxidation. Siderite was tested in thermogravimetric analysis (TGA) and in a 1 kW fixed-bed reactor. The raw siderite ore was stable for over 50 consecutive cycles at operating temperatures of 500–600 °C. However, the initial hydrogen storage capacity depletes in the first 15 cycles and then stabilizes. A hydrogen release step should take place between the temperatures of 100 and 500 °C, while temperatures above 500 °C would increase the energy consumption and potentially decrease the cycling stability [6].

Isothermal and non-isothermal reductions of MoO_2 powder (to Mo) by pure hydrogen were studied by Dang et al. [27]. They observed a complete reduction to metal (Mo) in both modes of reduction. Their MoO_2 powder reduction kinetics model has been proposed, which incorporates various factors, e.g., time, temperature and hydrogen content. Good

agreements were found between the experimentally measured and theoretically calculated results. A similar study was performed by Wang et al. [28], which focused on the hydrogen reduction of ultrafine MoO_2 powder at the temperature range between 863 (590) and 1023 K (750 °C). They focused on various reaction mechanisms and models (e.g., chemical vapor transport mechanism, nucleation and growth model, diffusion model) and their validity at different reaction conditions. The calculations of Brinkman et al. [6] revealed that a reduction of MoO_2 would be favorable at temperatures above 590 °C, while the oxidation of Mo should be induced at temperatures below 1110 °C.

WO_3 was completely reduced with hydrogen to W at 875 °C via the formation of two intermediate products: $WO_{2.72}$ (at 520 °C) and WO_2 (at 600 °C) [29]. The initial stage of the WO_3 reduction was found to be dominated by the formation of WO_2, and it was found to be affected by strong autocatalytic effects associated with the beginning of formation of W. Brinkman et al. [6] found out that the reduction of $WO_{2.722}$ would be favorable at temperatures above 590 °C, and the oxidation of W would be induced at temperatures below 640 °C.

More details about the hydrogen reduction of non-ferrous metal oxides with a focus on reduction kinetics and mechanisms were summarized by Rukini et al. [30]. Studies on the oxidation of metals with water vapor are on the other hand rare in the current literature. More research efforts should therefore be focused on the oxidation of metals with water vapor.

The hydrogen storage densities and energy–enthalpy ratios for the four viable metals are presented in Table 4. Manganese has the highest hydrogen storage density and energy–enthalpy ratio amongst the selected metals.

Table 4. Hydrogen storage densities and energy–enthalpy ratios of Mn, Fe, Mo and W.

Metal	SD_1 (/)	SD_2 (/)	*EER* (/)
Mn	0.0734	0.0443	15.73
Fe	0.0541	0.0365	8.69
Mo	0.0420	0.0305	5.43
W	0.0329	0.0254	7.30

Since manganese has a favorable combination of thermodynamic parameters of hydrogen reduction, with the lowest equilibrium reaction temperature amongst the ones above 25 °C, combined with the highest hydrogen storage density and energy–enthalpy ratio, it has the largest theoretical potential for hydrogen storage with the reaction of a reversible reduction and oxidation of metal oxides and metals. In addition to this, manganese is a fairly abundant metal which constitutes roughly 0.1 percent of the Earth's crust, making it the 12th most abundant element [31]. About 90 percent of Mn is currently consumed by the steel industry [31]. Manganese is the 4th most used metal on Earth (by mass), behind iron, aluminum and copper [32]. Therefore, Mn is a common commodity with an affordable price [33,34], which would enable its large-scale deployment for thermochemical hydrogen storage in the future energy landscape. Manganese was for example also considered as an affordable energy storage material via reversible plating/stripping by Chu and Yu [35].

Iron has the second highest thermochemical hydrogen storage potential, and it has been studied the most for this purpose, which is already described in the introduction. An idea of using of ferromanganese alloy(s), which is commonly used in steelmaking, for thermochemical hydrogen storage comes up, since both of the individual metals (Mn and Fe) exhibit high thermochemical hydrogen storage potentials. A combination of iron and manganese might produce favorable hydrogen storage results, especially if the materials would exhibit high thermal stability resistance to sintering.

Additional research efforts should be dedicated to the experimental testing of the cyclic reduction/oxidation of Mn, Fe, ferromanganese alloy(s), Mo and W. Even if it turns out that it is only possible and/or much more energy efficient (reduction at lower temperature)

to reversibly reduce/oxidize between two types of metal oxides, e.g., MnO_2 and MnO, this method could also be applicable for thermochemical hydrogen storage. The fluidized bed reactor (for smaller particles), fixed-bed reactor (for larger particles) or some other custom-made reactor solutions should be tested and optimized to enable deployment of the identified metals and their oxides as thermochemical hydrogen storage materials.

4. Conclusions

Our study is based on theoretical screening of all non-radioactive metals without lanthanides and their stable oxides for thermochemical hydrogen storage by the reduction of selected metal oxides and its subsequent release by metal oxidation with water vapor. We considered the reaction thermodynamics and thermal stability of the solid materials to select the viable candidates (metals/metal oxides). The viable materials were further analyzed in terms of their theoretical hydrogen storage performance.

Four viable elements of metals were identified: manganese (Mn), iron (Fe), molybdenum (Mo) and tungsten (W) with the potential for hydrogen storage via the reaction of the reversible reduction and oxidation of the metal oxides: MnO_2, Fe_2O_3, MoO_2 and WO_3. Their hydrogen storage densities are Mn > Fe > Mo > W, while their energy–enthalpy ratios follow the sequence Mn > Fe > W > Mo. Therefore, manganese has the largest theoretical potential for hydrogen storage with the reaction of reversible reduction and oxidation of metal oxides and metals, while its low equilibrium reaction temperature of 108.5 °C means that hydrogen release reaction should be performed in the narrow temperature window between the boiling point of water (100.0 °C) and the equilibrium reaction temperature (108.5 °C). The second place in hydrogen storage potential is occupied by iron, which has been studied extensively both for the thermochemical hydrogen storage on its own and also for the hydrogen reduction of iron ore, which plays a significant part in the iron and steel industry decarbonization. The remaining two elements (Mo and W) have according to our estimation much lower potential for thermochemical hydrogen storage and are also much less abundant (both in concentration around 1.5 ppm in Earth's crust). Therefore, Mo and W could be employed in some small-scale and/or niche applications, e.g., hydrogen storage in space.

Our short literature survey revealed that the reduction of various metal oxides with hydrogen was frequently studied and modeled, while there is a lack of work on the (re-)oxidation of metals with water vapor. Therefore, further research efforts are needed to experimentally test the identified viable metals (Mn, Fe, Mo and W) and their different oxides (e.g., MnO_2, Fe_2O_3, MoO_2 and WO_3) for cyclic reduction/oxidation capabilities. More laboratory scale tests would be appreciated for Mn, Mo and W, while pilot-scale experiments should be conducted mostly on Fe and Mn. Research in thermochemical hydrogen storage with ferromanganese alloy(s) might also produce promising results. Multiple different process conditions should be investigated, e.g., temperature, gas flow rate, particle size, type and size of a reactor, chemical composition and others. With optimization of the cyclic reduction/oxidation processes, the thermochemical hydrogen storage with the reversible reduction and oxidation of metal oxides and metals has the potential to become an economically feasible technology which can compete with other hydrogen storage technologies in the future decarbonized energy landscape with a large share of intermittent sources of power.

Author Contributions: Conceptualization, B.L. and J.V.; methodology, J.V.; formal analysis, J.V.; investigation, J.V.; resources, B.L.; data curation, J.V.; writing—original draft preparation, J.V.; writing—review and editing, B.L. and J.V.; visualization, J.V.; supervision, B.L.; funding acquisition, B.L. All authors have read and agreed to the published version of the manuscript.

Funding: B.L. thanks the support from the Slovenian Research and Innovation Agency through core funding P2-0152 and project funding J7-4638, N2-0291. B.L. acknowledges the support of the European Regional Development Fund for funding the H2GreenFUTURE project. B.L. also thanks for

support by the HyBReED programme, which is co-financed by the Republic of Slovenia, the Ministry of Higher Education, Science and Innovation and the European Union-NextGenerationEU.

Data Availability Statement: The raw data supporting the conclusions of this article will be made available by the authors on request.

Conflicts of Interest: The authors declare no conflicts of interest.

References

1. Sánchez-Diaz, C.; Monrabal, J.; González, D.; Alfonso, D.; Peñalvo-López, E. Experimental results of the hydrogen production control of a hydrogen energy buffer. *Int. J. Hydrogen Energy* **2015**, *40*, 5013–5024. [CrossRef]
2. Usman, M.R. Hydrogen storage methods: Review and current status. *Renew. Sustain. Energy Rev.* **2022**, *167*, 112743. [CrossRef]
3. Züttel, A. Hydrogen storage methods. *Naturwissenschaften* **2004**, *91*, 157–172. [CrossRef]
4. Klerke, A.; Christensen, C.H.; Nørskov, J.K.; Vegge, T. Ammonia for hydrogen storage: Challenges and opportunities. *J. Mater. Chem.* **2008**, *18*, 2304–2310. [CrossRef]
5. Räuchle, K.; Plass, L.; Wernicke, H.; Bertau, M. Methanol for renewable energy storage and utilization. *Energy Technol.* **2016**, *4*, 193–200. [CrossRef]
6. Brinkman, L.; Bulfin, B.; Steinfeld, A. Thermochemical hydrogen storage via the reversible reduction and oxidation of metal oxides. *Energy Fuels* **2021**, *35*, 18756–18767. [CrossRef]
7. Otsuka, K.; Kaburagi, T.; Yamada, C.; Takenaka, S. Chemical storage of hydrogen by modified iron oxides. *J. Power Sources* **2003**, *122*, 111–121. [CrossRef]
8. Lorente, E.; Peña, J.A.; Herguido, J. Separation and storage of hydrogen by steam-iron process: Effect of added metals upon hydrogen release and solid stability. *J. Power Sources* **2009**, *192*, 224–229. [CrossRef]
9. Hilde Lucassen, Iron-Based Hydrogen Storage, Wevolver. 2022. Available online: https://www.wevolver.com/article/iron-based-hydrogen-storage (accessed on 11 March 2024).
10. Gamisch, B.; Huber, L.; Gaderer, M.; Dawoud, B. On the kinetic mechanisms of the reduction and oxidation reactions of iron oxide/iron pellets for a hydrogen storage process. *Energies* **2022**, *15*, 8322. [CrossRef]
11. Thaler, M.; Hacker, V. Storage and separation of hydrogen with the metal steam process. *Int. J. Hydrogen Energy* **2012**, *37*, 2800–2806. [CrossRef]
12. Reed, J.J. *The NBS Tables of Chemical Thermodynamic Properties: Selected Values for Inorganic and C1 and C2 Organic Substances in SI Units*; National Institute of Standards and Technology: Gaithersburg, MD, USA, 1989. [CrossRef]
13. Schmitz, K.S. *Physical Chemistry: Concepts and Theory*; Elsevier: Amsterdam, The Netherlands, 2016.
14. Agbossou, K.; Chahine, R.; Hamelin, J.; Laurencelle, F.; Anouar, A.; St-Arnaud, J.-M.; Bose, T.K. Renewable energy systems based on hydrogen for remote applications. *J. Power Sources* **2001**, *96*, 168–172. [CrossRef]
15. Allison, J.; Bell, K.; Clarke, J.; Cowie, A.; Elsayed, A.; Flett, G.; Oluleye, G.; Hawkes, A.; Hawker, G.; Kelly, N. Assessing domestic heat storage requirements for energy flexibility over varying timescales. *Appl. Therm. Eng.* **2018**, *136*, 602–616. [CrossRef]
16. Dinker, A.; Agarwal, M.; Agarwal, G.D. Heat storage materials, geometry and applications: A review. *J. Energy Inst.* **2017**, *90*, 1–11. [CrossRef]
17. Barner, H.E.; Mantell, C.L. Kinetics of hydrogen reduction of manganese dioxide. *Ind. Eng. Chem. Process Des. Dev.* **1968**, *7*, 285–294. [CrossRef]
18. Brooks, C.S. The kinetics of hydrogen and carbon monoxide oxidation over a manganese oxide. *J. Catal.* **1967**, *8*, 272–282. [CrossRef]
19. De Bruijn, T.J.W.; Soerawidjaja, T.H.; De Jongt, W.A.; Van Den Berg, P.J. Modelling of the reduction of manganese oxides with hydrogen. *Chem. Eng. Sci.* **1980**, *35*, 1591–1599. [CrossRef]
20. Anacleto, N.; Ostrovski, O.; Ganguly, S. Reduction of manganese ores by methane-containing gas. *ISIJ Int.* **2004**, *44*, 1615–1622. [CrossRef]
21. Tatievskaya, E.P.; Antonov, V.K.; Chufarov, G.M. Rate of reduction of manganese oxides by hydrogen and by carbon monoxide. *Aad. Nauk SSSR* **1949**, *68*, 561–564.
22. Zieliński, J.; Zglinicka, I.; Znak, L.; Kaszkur, Z. Reduction of Fe_2O_3 with hydrogen. *Appl. Catal. A Gen.* **2010**, *381*, 191–196. [CrossRef]
23. Ma, Y.; Filho, I.R.S.; Bai, Y.; Schenk, J.; Patisson, F.; Beck, A.; van Bokhoven, J.A.; Willinger, M.G.; Li, K.; Xie, D. Hierarchical nature of hydrogen-based direct reduction of iron oxides. *Scr. Mater.* **2022**, *213*, 114571. [CrossRef]
24. Zhang, T.; Lei, C.; Zhu, Q. Reduction of fine iron ore via a two-step fluidized bed direct reduction process. *Powder Technol.* **2014**, *254*, 1–11. [CrossRef]
25. Guo, L.; Bao, Q.; Gao, J.; Zhu, Q.; Guo, Z. A review on prevention of sticking during fluidized bed reduction of fine iron ore. *ISIJ Int.* **2020**, *60*, 1–17. [CrossRef]
26. Bock, S.; Pauritsch, M.; Lux, S.; Hacker, V. Natural iron ores for large-scale thermochemical hydrogen and energy storage. *Energy Convers. Manag.* **2022**, *267*, 115834. [CrossRef]
27. Dang, J.; Zhang, G.-H.; Chou, K.-C. Study on kinetics of hydrogen reduction of MoO_2. *Int. J. Refract. Met. Hard Mater.* **2013**, *41*, 356–362. [CrossRef]

28. Wang, L.; Zhang, G.-H.; Wang, J.-S.; Chou, K.-C. Study on hydrogen reduction of ultrafine MoO_2 to produce ultrafine Mo. *J. Phys. Chem. C* **2016**, *120*, 4097–4103. [CrossRef]
29. Fouad, N.E.; Attyia, K.M.E.; Zaki, M.I. Thermogravimetry of WO_3 reduction in hydrogen: Kinetic characterization of autocatalytic effects. *Powder Technol.* **1993**, *74*, 31–37. [CrossRef]
30. Rukini, A.; Rhamdhani, M.A.; Brooks, G.A.; Van den Bulck, A. Metals production and metal oxides reduction using hydrogen: A review. *J. Sustain. Metall.* **2022**, *8*, 1–24. [CrossRef]
31. Cannon, W.F. *Manganese: It Turns Iron into Steel (and Does So Much More)*; US Geological Survey: Reston, VA, USA, 2014.
32. International Manganese Institute, ABOUT MANGANESE, (n.d.). Available online: https://www.manganese.org/what-is-manganese/ (accessed on 28 March 2024).
33. U.S. Geological Survey. Metal Prices in the United States through 2010: U.S. Geological Survey Scientific Investigations Report 2012–5188, 2013. 204p. Available online: http://pubs.usgs.gov/sir/2012/5188 (accessed on 28 March 2024).
34. Bourriquen, F.; Rockstroh, N.; Bartling, S.; Junge, K.; Beller, M. Manganese-Catalysed Deuterium Labelling of Anilines and Electron-Rich (Hetero) Arenes. *Angew. Chem. Int. Ed.* **2022**, *61*, e202202423. [CrossRef]
35. Chu, X.; Yu, M. Reversible manganese plating/stripping. *Joule* **2024**, *8*, 566–568. [CrossRef]